Synthesis, Structure, and Reactivity of [(dfepe)Pt(μ-H)]$_2$. An Unusual Example of Conformational Polymorphism

Byron L. Bennett and Dean M. Roddick*

Department of Chemistry, Box 3838, University of Wyoming, Laramie, Wyoming 82071

Received February 5, 1996[⊗]

Treatment of the methyl complex (dfepe)Pt(Me)(O_2CCF_3) (dfepe = $(C_2F_5)_2PCH_2CH_2P(C_2F_5)_2$) with 1 atm of H_2 in acetone at 20 °C cleanly affords the hydride-bridged dimer [(dfepe)Pt(μ-H)]$_2$ (**1**), which crystallizes in both green (**1a**, monoclinic) and purple (**1b**, orthorhombic) forms. Diffraction data indicate that **1a** and **1b** are conformational polymorphs which primarily differ in the degree of rotation about the Pt−Pt bond (interchelate angle = 7° (**1a**), 49° (**1b**)) and intermolecular crystal packing. DSC experiments reveal a mildly exothermic (0.51 kJ mol^{-1}) irreversible phase transition from **1a** to **1b** at 91 °C (mp of **1b** = 112 °C). In CH_2Cl_2, **1** exhibits a distinctive d$\pi \rightarrow$ dσ^* transition at 428 nm ($\epsilon \sim 4000$ mol^{-1} cm^{-1}) and a reversible redox couple at +0.63 V (CH_2Cl_2, vs SCE). [(dfepe)Pt(μ-H)]$_2$ serves as a versatile precursor to (dfepe)Pt^0 compounds: exposure of acetone solutions of **1** to 1 atm of C_2H_4, C_2F_4, or CO results in clean conversions to (dfepe)Pt(η^2-C_2H_4) (**2**), (dfepe)Pt(η^2-C_2F_4) (**3**), and (dfepe)Pt(CO) (**4**) (ν(CO) = 2044 cm^{-1}), respectively. With the exception of **3**, these Pt(0) derivatives readily revert to the hydride dimer under 1 atm of H_2 at ambient temperature. Under 2 atm of CO, the reversible formation of (dfepe)Pt(CO)$_2$ (**5**) from **4** is observed. X-ray data for **1a**: a = 23.527(5) Å, b = 10.451(2) Å, c = 16.623(3) Å, β = 110.20(3)°, monoclinic, $C2/c$, Z = 4, R = 0.0670. Data for **1b**: a = 13.354(3) Å, b = 16.232(3) Å, c = 18.525(4) Å, orthorhombic, $Pccn$, Z = 4, R = 0.0423.

Introduction

Platinum phosphine hydride complexes [$(R_3P)_2M(H)_x]_n$ exhibit intriguing differences in structure and reactivity properties that are highly dependent on the nature of the phosphine ligand used. For chelating phosphine derivatives $R_2P(CH_2)_nPR_2$ (n = 1−3), facile interconversions between monomeric *cis*-dihydride and dimeric hydride derivatives (P−P)Pt(H)$_2$ and [(P−P)Pt(H)]$_2$ whose relative stabilities are dependent on both chelate bite angle and the steric influence of the terminal alkyl or aryl groups have been reported.[1−3] For the dimeric hydrides in particular, Andersen recently noted a progression of symmetrical bridging, semibridging, and terminal hydride coordination upon descending the nickel triad.[1] Our recent studies of electron-poor (dfepe)Pt^{II} (dfepe = $(C_2F_5)_2PCH_2CH_2P(C_2F_5)_2$) systems revealed chemistry distinctly different from that of donor phosphine analogues.[4] As part of this work, we report here the synthesis and structural characterization of [(dfepe)Pt(μ-H)]$_2$, an unusual hydride-bridged platinum dimer which exhibits conformational polymorphism.

Treatment of the methyl complex (dfepe)Pt(Me)(O_2CCF_3)[4b] with 1 atm of H_2 in acetone at 20 °C cleanly affords [(dfepe)Pt(μ-H)]$_2$ (**1**) in good yield (eq 1). Complex **1** is completely air-stable in the solid state. Although no intermediates were observed by NMR, an initial displacement of $CF_3CO_2^-$ by H_2 to form a transient Pt(II) dihydrogen species [(dfepe)Pt(η^2-H_2)Me]$^+$ is a reasonable possibility.[5] Rapid deprotonation of this

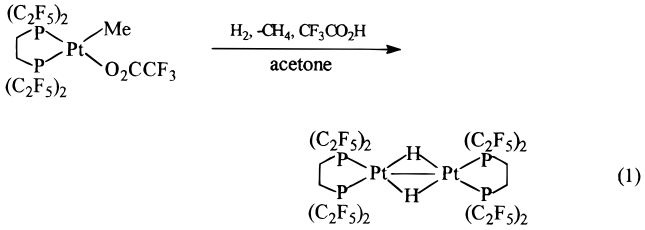

(1)

intermediate followed by methane elimination and subsequent hydrogen addition would give the observed product. Unlike donor phosphine analogues, which are readily protonated to form $P_4Pt_2H_3^+$ derivatives, **1** does not protonate in the presence of excess CF_3CO_2H. Consistent with those of other dimeric platinum hydride complexes, room-temperature ^{1}H NMR spectra of **1** show a distinctive "quintet of quintet" hydride resonance at 3.55 ppm ($^1J_{PtH}$ = 737 Hz, $^2J_{PH}$ = 47 Hz) in an approximately 1:8:18:8:1 intensity ratio that is diagnostic for chemical equivalence of the two platinum centers with ^{195}Pt present in natural abundance with coupling to four chemically equivalent phosphorus nuclei.[1,3b] ^{31}P spectra of **1** are complicated by $^2J_{PF}$ coupling to diastereotopic CF_2 groups. In fluorine-decoupled ^{31}P spectra, however, the dfepe resonance appears as a broadened triplet ($^2J_{PH}$ = 47 Hz) due to coupling with two equivalent hydride ligands with two sets of ^{195}Pt satellite doublets arising from coupling to the attached ($^1J_{PtP}$ = 3883 Hz) and neighboring ($^2J_{PtP}$ = 304 Hz) platinum centers. The $^2J_{PH}$ coupling to the dfepe ligand backbone is not resolved. No significant changes are observed in the ^{1}H and ^{31}P NMR spectra down to −90 °C.

Since NMR data do not distinguish between terminal and bridged hydride coordination in highly fluxional systems,[1,7] a crystallographic study of **1** was initiated. Interestingly, the

[⊗] Abstract published in *Advance ACS Abstracts,* July 15, 1996.

(1) Schwartz, D. J.; Andersen, R. A. *J. Am. Chem. Soc.* **1995**, *117*, 4014.
(2) (a) Carmichael, D.; Hitchcock, P. B.; Nixon, J. F.; Pidcock, A. *J. Chem. Soc., Chem. Commun.* **1988**, 1554. (b) Scrivanti, A.; Campostrini, R.; Carturan, G. *Inorg. Chim. Acta* **1988**, *142*, 187. (c) Clark, H. C.; Hampden-Smith, M. J. *J. Am. Chem. Soc.* **1986**, *108*, 3829.
(3) (a) Otsuka, S. *J. Organomet. Chem.* **1980**, *200*, 191. (b) Tulip, T. H.; Yamagata, T.; Yoshida, T.; Wilson, R. D.; Ibers, J. A.; Otsuka, S. *Inorg. Chem.* **1979**, *18*, 2239. (c) Yoshida, T.; Yamagata, T.; Tulip, T. H.; Ibers, J. A.; Otsuka, S. *J. Am. Chem. Soc.* **1978**, *100*, 2063.
(4) (a) Merwin, R. K.; Schnabel, R. C.; Koola, J. D.; Roddick, D. M. *Organometallics* **1992**, *11*, 2972. (b) Bennett, B. L.; Birnbaum, J.; Roddick, D. M. *Polyhedron* **1995**, *14*, 187.

(5) Since no reaction between (dfepe)Pt(Me)$_2$ and H_2 takes place at temperatures up to 150 °C,[6] the direct oxidative addition of H_2 to 16 e$^-$ (dfepe)Pt(Me)(O_2CCF_3) to form a Pt(IV) intermediate (dfepe)Pt(Me)(O_2CCF_3)H_2 does not appear to be an energetically accessible reaction pathway.

(6) Merwin, R. K.; Roddick. D. M. Unpublished results.

S0020-1669(96)00126-7 CCC: $12.00

Table 1. Crystallographic Data for [(dfepe)Pt(μ-H]$_2$ Polymorphs (**1a**) and (**1b**)

	1a	**1b**
empirical formula	$C_{20}H_{10}F_{40}P_4Pt_2$	$C_{20}H_{10}F_{40}P_4Pt_2$
fw	1524.3	1524.3
space group	*C*2/*c* (No. 15)	*Pccn* (No. 56)
a (Å)	23.527(5)	13.354(3)
b (Å)	10.451(2)	16.232(3)
c (Å)	16.623(3)	18.525(4)
β (deg)	110.20(3)	
V (Å^3)	3835.8(13)	4015.6(15)
Z	4	4
T (°C)	−100	−100
λ (Å)	0.710 73	0.710 73
D_{calc} (g cm^{-3})	2.640	2.521
μ (cm^{-1})	76.68	73.25
transm coeff	0.55−1.92	0.83−1.23
$R(F)$ ($F_o > 4\sigma(F_o)$),[a] %	6.70	4.23
$R_w(F)$ ($F_o > 4\sigma(F_o)$),[b] %	16.75 (for $R_w(F^2)$)	4.87

[a] $R(F_o) = \sum(|F_o| - |F_c|)/\sum|F_o|$. [b] $R_w(F_o) = \sum(w^{1/2}(|F_o| - |F_c|))/\sum(w^{1/2}|F_o|)$.

Table 2. Atomic Coordinates ($\times 10^4$) and Equivalent Isotropic Displacement Parameters (Å^2 $\times$ 10^3) for [(dfepe)Pt(μ-H)]$_2$ (**1a**) and (**1b**)

atom	*x*	*y*	*z*	*U*(eq)[a]
		Complex **1a**		
Pt(1)	618(1)	3652(1)	2623(1)	15(1)
P(1)	1305(2)	5155(3)	2714(2)	19(1)
P(2)	1298(2)	2195(3)	2593(2)	19(1)
		Complex **1b**		
Pt(1)	1857(1)	6853(1)	1462(1)	16(1)
P(1)	292(2)	6635(1)	1128(1)	18(1)
P(2)	1930(2)	5556(1)	1820(1)	20(1)

[a] *U*(eq) is defined as one-third of the trace of the orthogonalized $\mathbf{U}_{ij}$ tensor.

nature of the crystals obtained is solvent-dependent: green plates (**1a**) are obtained from saturated benzene solutions whereas purple needles (**1b**) are formed from dichloromethane. The equivalence of solution NMR data for both **1a** and **1b** and the absence of any residual solvents of crystallization suggested that **1a** and **1b** are true polymorphs. Indeed, DSC experiments reveal that **1a** undergoes a mildly exothermic irreversible phase transition (0.51 kJ mol^{-1}) to **1b** at 91 °C; a corresponding change in color from **1a** to **1b** is observed during this exotherm. The melting range of the phase-changed material (110−112 °C) is also essentially identical to that of **1b**. Interestingly, this phase transition may also be induced by mechanical shock: cutting crystals of **1a** with a razor blade to obtain suitable crystals for X-ray analysis in several instances resulted in a spontaneous phase transition from **1a** to **1b**.

The structures of both crystal forms of **1** were obtained at −100 °C. A summary of data collection parameters and a listing of selected atom fractional coordinates and equivalent isotropic thermal parameters are presented in Tables 1 and 2, respectively. Bond distances and angles are given in Table 3. Despite differences in overall crystal symmetry (**1a**, *C2/c*; **1b**, *Pccn*), the molecules in each of these settings reside on crystallographic 2-fold axes perpendicular to the Pt−Pt bond which relate the halves of the dimeric unit. As shown in Figures 1 and 2, the principal structural difference is the relative dfepe chelate

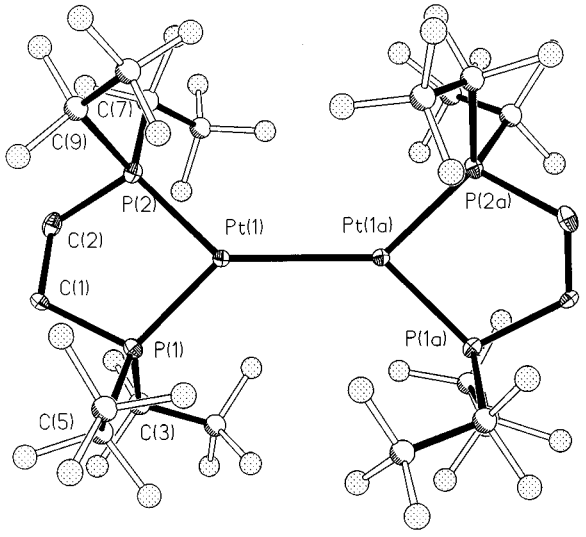

Figure 1. Molecular structure of **1a** (green plates) with atom-labeling scheme (30% probability ellipsoids; unlocated metal hydride ligands and idealized dfepe backbone hydrogen atoms omitted).

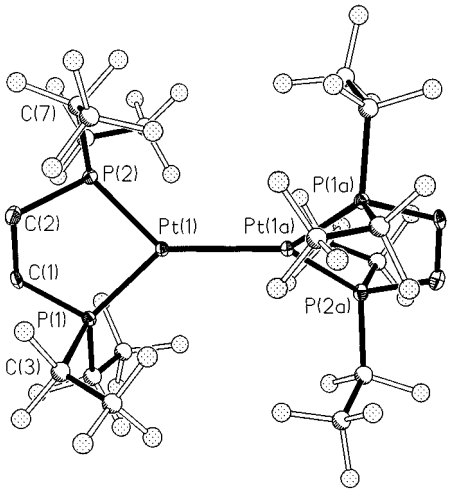

Figure 2. Molecular structure of **1b** (purple needles) with atom-labeling scheme (30% probability ellipsoids; unlocated metal hydride ligands and idealized dfepe backbone hydrogen atoms omitted).

Table 3. Selected Bond Lengths (Å) and Angles (deg) for [(dfepe)Pt(μ-H)]$_2$ (**1a**) and (**1b**)

	1a	**1b**
	Bond Lengths	
Pt(1)−P(1)	2.221(3)	2.208(2)
Pt(1)−P(2)	2.221(3)	2.210(2)
Pt(1)−Pt(1a)	2.791(1)	2.714(1)
	Bond Angles	
P(1)−Pt(1)−P(2)	88.5(1)	88.5(1)
P(1)−Pt(1)−Pt(1a)	134.9(1)	136.3(1)
P(2)−Pt(1)−Pt(1a)	135.9(1)	135.2(1)
	Torsional Angles	
P(1)−Pt(1)−Pt(1a)−P(1a)	−5.4	−132.1
P(1)−Pt(1)−Pt(1a)−P(2a)	−172.7	49.2
P(2)−Pt(1)−Pt(1a)−P(2a)	19.9	−129.6

conformation about the Pt−Pt bond: referring to planes defined by the Pt and dfepe phosphorus atoms, **1a** exhibits an essentially eclipsed chelate arrangement (interplanar angle = 7°) whereas **1b** is staggered (49°). The dihedral angle for **1b** is intermediate between values reported for [(dcypp)Ni(μ-H)]$_2$ (63°)[8] and [(dippp)Pd(μ-H)]$_2$ (24°)[9] and appears to represent a steric

(7) No IR bands attributable to ν(Pt−H) were observed for **1** in solution or in the solid state. Although the absence of terminal ν(Pt−H) bands in the 1900 cm^{-1} region is often cited as evidence for M$_2$(μ-H)$_2$ coordination, this negative evidence is not compelling since in our experience (dfepe)M(H)$_x$ complexes frequently have very weak or absent terminal hydride modes. No ν(Pt−D) modes were identified in IR spectra of **1a**-d_2.

(8) Barnett, B. L.; Krüger, C.; Tsay, Y.-H.; Summerville, R. H.; Hoffmann, R. *Chem. Ber.* **1977**, *110*, 3900.

minimum with an optimal meshing of opposing dfepe ligand CF_3 groups. Although the hydride ligands in **1a** and **1b** were not located, all the observed Pt−Pt−P angles are nearly identical (134.9−136.3°) and are consistent with bridged rather than terminal hydride coordination. The Pt−Pt bond lengths observed for **1a** (2.791(1) Å) and **1b** (2.714(1) Å) are substantially longer than values reported for unbridged Pt(I)−Pt(I) bonds (2.53−2.63 Å)[1,10] and are more in line with $Pt_2(\mu\text{-}H)_2$ structures such as $(dtbpp)_2Pt_2(\mu\text{-}H)_2H^+$ (2.768(2) Å).[3b] The longer metal−metal distance found for the eclipsed isomer **1a** may be at least partly attributed to increased steric interactions between the dfepe ligands (closest intramolecular F−F contacts: 2.80 Å (**1a**), 3.03 Å (**1b**)).

The conformational polymorphism observed for **1** is quite unusual. Although this phenomenon is fairly common in organic systems,[11] relatively few organometallic examples have been reported.[12] A recent unusual example of distortional isomerism has been reported for $[Cp^*Ru(\mu\text{-}Cl)Cl]_2$, which exhibits independent diamagnetic (Ru−Ru = 2.93 Å) and paramagnetic (Ru−Ru = 3.75 Å) structural isomers in the same crystal lattice.[13] Examples of solid-state rotational isomerism for dimeric metal systems $[(dimen)_4M_2]^{2+}$ (M = Rh, Ir) and $Os_2Br_8^{2-}$ have also appeared;[14,15] however, unlike these ionic systems the rotamerism of $[(dfepe)Pt(\mu\text{-}H)]_2$ is not dictated by counterion effects. Calculations for $L_4Ni_2(\mu\text{-}H)_2$ indicate that there is only a modest energetic preference for a fully-eclipsed geometry and a very soft potential energy surface for rotation about the metal−metal axis.[8]

Crystal packing diagrams for **1a** and **1b** are informative (Figure 3). Despite the modest energetics associated with the solid state transition between these polymorphs, the packing motifs are very different. In **1a**, all molecules are oriented identically with respect to the unit cell axes in staggered two-dimensional arrays. In contrast, **1b** adopts a fully alternating pattern with nearest neighbors canted 78° with respect to the Pt−Pt axes. Crystal density comparisons normally provide a rough measure of polymorph packing efficiencies. Interestingly, although the monoclinic crystal form **1a** is thermodynamically less stable than **1b**, it is actually the densest phase (**1a**, 2.640 g/cm^3, **1b**, 2.521 g/cm^3), suggesting that the lower intermolecular packing efficiency in **1b** is compensated by a relief of intramolecular nonbonded repulsions.

$[(dfepe)Pt(\mu\text{-}H)]_2$ may be formally described as a coordinatively-saturated d^9−d^9 complex with 3-center 2e$^-$ hydride bridges and a Pt(I)−Pt(I) single bond. Physical data are consistent with this formulation. UV−vis solution spectra of **1** exhibit a distinctive visible band at 428 nm (CH_2Cl_2; $\epsilon \sim 4000$ mol^{-1} cm^{-1}), which is tentatively attributed to a metal-based $d\pi \rightarrow d\sigma^*$ transition (Figure 4).[16] For comparison, the donor phosphine complex $[(^tBu)_2PCH_2CH_2P(^tBu)_2Pt(H)]_2$ exhibits a corresponding visible transition at 409 nm (CH_2Cl_2, $\epsilon \sim 1700$ mol^{-1} cm^{-1}). Although $[(dfepe)Pt(\mu\text{-}H)]_2$ does not exhibit reversible electrochemical behavior in coordinating solvents such as thf or acetonitrile, cyclovoltammetry in dichloromethane reveals a one-electron oxidation at +0.63 V vs SCE (0.1 M $[Bu_4N]^+ClO_4^-$, 100 mV s^{-1}) that is attributed to a Pt−Pt(I)/Pt−Pt(II) redox couple. The reversibility of this redox process was confirmed by a linear plot of (scan rate)$^{1/2}$ vs peak current ($R^2 = 0.999$). Any destabilization accompanying the removal of an electron from the $Pt_2(\mu\text{-}H)_2$ bonding framework is apparently mitigated by the presence of hydride

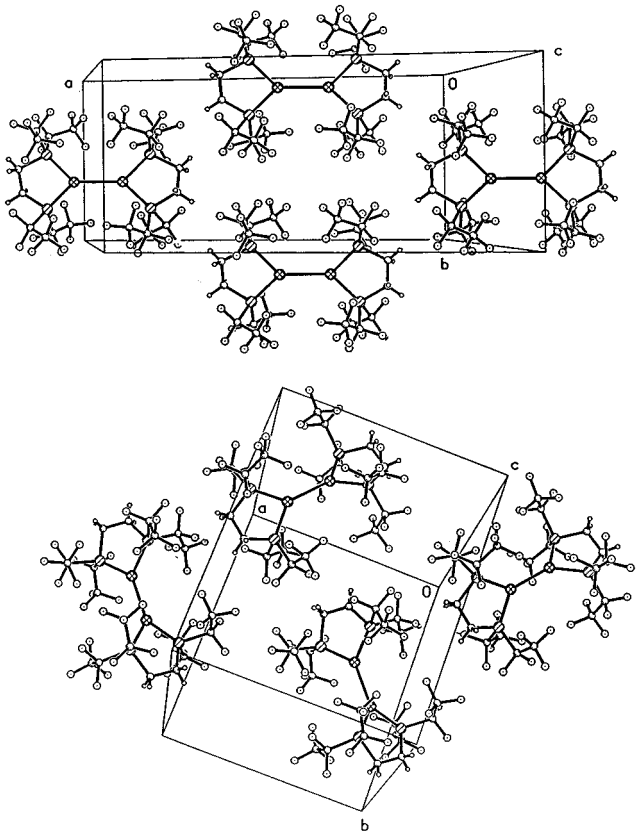

Figure 3. Crystal packing diagrams for hydride dimers **1a** (top) and **1b** (bottom), showing the parallel and staggered intermolecular orientations for these molecules.

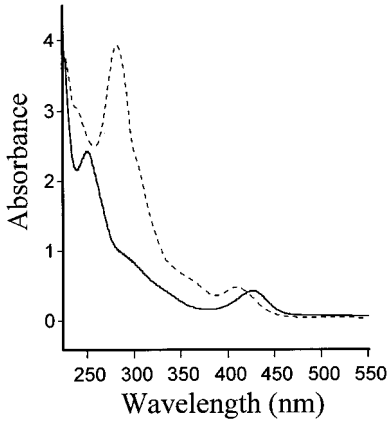

Figure 4. Comparison of electronic absorption spectra of $[(dfepe)Pt(\mu\text{-}H)]_2$ (**1**) (1.02×10^{-4} M, solid line) and $[(^tBu)_2PCH_2CH_2P(^tBu)_2Pt(H)]_2$ (5.18×10^{-4} M, dashed line).

(9) Fryzuk, M. D.; Lloyd, B. R.; Clentsmith, G. K. B.; Rettig, S. J. *J. Am. Chem. Soc.* **1994**, *116*, 3804.
(10) (a) Couture, C.; Farrar, D. H.; Fisher, D. S.; Gukathasan, R. R. *Organometallics* **1987**, *6*, 532. (b) Modinos, A.; Woodward, P. *J. Chem. Soc., Dalton Trans.* **1975**, 1516.
(11) (a) *Organic Solid State Chemistry*; Desiraju, G. R., Ed.; Elsevier Science Publishing: New York, 1987; Chapters 12 and 13. (b) Gavezzotti, A.; Filippini, G. *J. Am. Chem. Soc.* **1995**, *117*, 12299. (c) Gavessotti, A.; Simonetta, M. *Chem. Rev.* **1982**, *82*, 1.
(12) (a) Braga, D.; Grepioni, F.; Calhorda, M. J.; Veiros, L. F. *Organometallics* **1995**, *14*, 1992. (b) Braga, D.; Grepioni, F.; Dyson, P. J.; Johnson, B. F. G.; Frediani, P.; Bianchi, M.; Piacenti, F. *J. Chem. Soc., Dalton Trans.* **1992**, 2565.
(13) Koelle, U.; Lueken, H.; Handrick, K.; Schilder, H.; Burdett, J. K.; Balleza, S. *Inorg. Chem.* **1995**, *34*, 6273.
(14) Exstrom, C. L.; Britton, D.; Mann, K. R.; Hill, M. G.; Miskowski, V. M.; Schaefer, W. P.; Gray, H. B.; Lamanna, W. M. *Inorg. Chem.* **1994**, *33*, 2799.
(15) Gross, C. L.; Wilson, S. R.; Girolami, G. S. *Inorg. Chem.* **1995**, *34*, 2582.
(16) The presence of hydride bridges complicates the assignment. For d^9−d^9 systems without bridging ligands, see: Dulebohn, J. I.; Ward, D. L.; Nocera, D. G. *J. Am. Chem. Soc.* **1990**, *112*, 2969.

Scheme 1

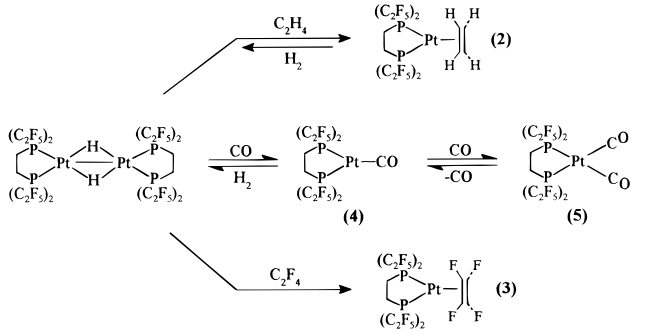

bridges. Significantly, cyclovoltammetric studies of $[(^tBu)_2PCH_2CH_2P(^tBu)_2Pt(H)]_2$, a molecule which has a terminal hydride ground state structure, did not show reversible redox behavior.

In addition to the intriguing physical properties of [(dfepe)Pt(μ-H)]$_2$, this complex serves as a versatile precursor to (dfepe)Pt^0 compounds. For example, exposure of acetone solutions of **1** to 1 atm of C_2H_4, C_2F_4, or CO results in clean conversions to (dfepe)Pt(η^2-C_2H_4) (**2**), (dfepe)Pt(η^2-C_2F_4) (**3**), and (dfepe)Pt(CO) (**4**, ν(CO) = 2044 cm^{-1}), respectively (Scheme 1). The isolation of a monocarbonyl adduct **4** contrasts with the carbonylation of the donor phosphine chelate complex $[(^tBu)_2PCH_2CH_2CH_2P(^tBu)_2Pt]_2$, which affords only the dicarbonyl derivative, $(^tBu)_2PCH_2CH_2CH_2P(^tBu)_2Pt(CO)_2$. Monitoring the reaction of **1** under 2 atm of CO in acetone by IR however revealed a complete conversion of initially-formed **4** to the dicarbonyl complex (dfepe)Pt(CO)$_2$ (**5**) after 1 h; **5** could not be isolated because of the facile loss of CO and reversion to **4**. The substantially higher ν(CO) values observed for **5** (2073, 2038 cm^{-1}) compared to those for $(^tBu)_2PCH_2CH_2CH_2P(^tBu)_2Pt(CO)_2$ (1960, 1912 cm^{-1})[3c] are consistent with the very electron-poor nature of the (dfepe)Pt moiety and the decreased stability of **5** relative to **4**.

In light of the above carbonylation results, we anticipated a reduced binding affinity of (dfepe)Pt toward a strongly electron-withdrawing tetrafluoroethylene ligand relative to electron-donating ethylene.[17] Nevertheless, (dfepe)Pt(η^2-C_2F_4) is considerably more stable than (dfepe)Pt(η^2-C_2H_4) and, unlike the ethylene adduct, does not readily exchange with free olefin. The orientation of the C_2F_4 ligand with respect to the plane defined by the dfepe phosphorus atoms and the platinum center is of interest. Previous structural and spectroscopic studies of L_2Pt(η^2-C_2F_4) complexes have shown that an in-plane orientation of the fluoro olefin ligand is preferred.[18] In particular, ^{19}F NMR data for *cis*-$(R_3P)_2$Pt(η^2-C_2F_4) complexes exhibit temperature-independent $A_2A'_2XX'$ coupling patterns consistent with a rigid in-plane metallacyclopropane formulation. Unlike those for previously reported L_2Pt(η^2-C_2F_4) complexes, however, ^{19}F NMR data for **3** show a simple triplet with platinum satellites at -125.8 ppm ($^3J_{FP}$ = 43 Hz, $^2J_{PtF}$ = 297 Hz), which suggests either a static olefin coordination perpendicular to the (dfepe)Pt plane or free olefin rotation on the NMR time scale.

The ethylene adduct **2** is much less stable than its fluorinated analogue and undergoes rapid ligand exchange on the NMR time scale with free ethylene at 20 °C. In the absence of excess free C_2H_4, the coordinated ethylene appears in ^{1}H NMR spectra as a broad singlet at δ 2.96 with a two-bond ^{195}Pt coupling of 68 Hz. In contrast to (dfepe)Pt(η^2-C_2F_4), whose formation is irreversible, both **2** and **4** are very labile and readily convert back to the hydride dimer **1** under 1 atm of H_2.

(17) A weaker binding affinity of C_2F_4 relative to C_2H_4 has been noted for electron-poor Ni(0) phosphite systems: Tolman, C. A. *J. Am. Chem. Soc.* **1974**, *96*, 2780.

(18) (a) Russell, D. R.; Tucker, P. A. *J. Chem. Soc., Dalton Trans.* **1975**, 1752. (b) Kemmitt, R. D. W.; Moore, R. D. *J. Chem. Soc. A* **1971**, 2472. (c) Green, M.; Osborn, R. B. L.; Rest, A. J.; Stone, F. G. A. *J. Chem. Soc. A* **1968**, 2525.

Summary

In the context of previous $[(R_3P)_2M(H)_x]_n$ chemistry, [(dfepe)Pt(μ-H)]$_2$ differs in both its structural and chemical properties. Unlike air-sensitive electron-rich donor phosphine analogues, the electron-withdrawing dfepe ligand in **1** induces enhanced air stability and lowered metal basicity. The preference for bridged-hydride coordination in **1** differs from the case of Andersen's structurally characterized $[(P\text{-}P)Pt(H)]_2$ systems. Although terminal hydride coordination in the latter systems was tentatively rationalized in terms of relativistic effects, it is clear from the highly fluxional nature of these systems that the energetic preferences must be quite small. We suggest that the preference for 3-center 2e$^-$ hydride bridges and a corresponding formal 18-electron metal valency in **1** may reflect the increased electrophilicity of the platinum centers. The conformational polymorphism exhibited by **1** is a rare example of this phenomenon in organometallics. As is generally the case, polymorphism in this system stems from a subtle interplay between conformation energetics and both intra- and intermolecular nonbonded interactions.

The different electronic properties of the (dfepe)Pt moiety indicated for **1** carry over into monomeric (dfepe)Pt^0 chemistry. In addition to decreased CO binding affinities, the bonding between platinum and the strong acceptor olefin C_2F_4 appear to be significantly altered and warrant further study. Structural, spectroscopic, and competitive ligand exchange studies of these new electron-poor platinum(0) systems are currently in progress.

Experimental Section

General Procedures. All manipulations were conducted under an atmosphere of nitrogen using Schlenk, high-vacuum-line, and/or glovebox techniques. Dry, oxygen-free solvents were vacuum-distilled prior to use. Elemental analyses were performed by Desert Analytics (Tucson, AZ). Infrared spectra were recorded on a Mattson Cygnus 100 or Perkin-Elmer 1600 FTIR instrument as Nujol mulls, unless otherwise noted. NMR spectra were obtained with a JEOL GSX-270 or GSX-400 instrument. ^{19}F spectra were referenced to CF_3CO_2Et as an external standard (-75.32 ppm vs $CFCl_3$ with downfield chemical shifts taken to be positive). ^{31}P spectra were referenced to a 85% H_3PO_4 external standard. (dfepe)Pt(Me)(O_2CCF_3) was prepared as described previously.[4b]

[(dfepe)Pt(μ-H)]$_2$. One atm of H_2 was admitted to a 25 mL flask containing 0.132 g (0.148 mmol) of (dfepe)Pt(Me)(O_2CCF_3) in 5 mL of acetone at ambient temperature. After 72 h, the volatiles were removed, the residue was dissolved in 5 mL of petroleum ether, and the solution was cooled to -78 °C. Cold filtration of the resulting filtrate and drying under vacuum afforded 0.080 g (70%) of crystalline green **1a** (mp (after phase change) 110−112 °C). Crystalline purple **1b** (mp 111−113 °C) was obtained by recrystallization of samples of **1a** from dichloromethane. Anal. Calcd for $C_{20}H_{10}F_{40}P_4Pt_2$ (**1a**): C, 15.74; H, 0.65. Found: C, 15.96; H, 1.08. Found for **1b**: C, 15.94; H, 0.62. IR (benzene, cm^{-1}): 1304 (s), 1295 (sh), 1225 (vs), 1124 (s), 1099 (sh), 958 (m), 803 (w). ^{1}H NMR (benzene-d_6, 400 MHz, 27 °C): δ 3.55 (pp, $^1J_{PtH}$ = 737 Hz, $^2J_{PH}$ = 47 Hz, 2H; Pt(μ-H)), 1.75 (m, 8H; PCH_2). {^{19}F}^{31}P NMR (benzene-d_6, 161.7 MHz, 23 °C): δ 87.7 (t, $^2J_{PH}$ = 47 Hz, $^1J_{PtP}$ = 3883 Hz, $^2J_{PPt}$ = 304 Hz). ^{19}F NMR (benzene-d_6, 376.05 MHz, 20 °C): δ -79.7 (s, 12F; $CF_2C\mathbf{F}_3$), -110.7 to -114.4 (m, 8F; $C\mathbf{F}_2CF_3$).

(dfepe)Pt(η^2-C_2H_4) (2). Complex **2** was generated *in situ* owing to the facile loss of ethylene at ambient temperatures. To a septum-capped 5 mm NMR tube charged with 5 mg of **1** in acetone-d_6 under N_2 was added 5 mL of ethylene gas via syringe. The solution became light yellow upon mixing. Initial NMR spectra under excess ethylene

revealed only an exchange-broadened C_2H_4 resonance. Removal of all volatiles and addition of fresh solvent yielded a sample of essentially pure **2**. ^{1}H NMR (400 MHz, acetone-d_6, 25 °C): δ 2.96 (br s, $^2J_{PtH}$ = 68 Hz, 4H; η^2-C_2H_4), 2.72 (m, 4H; PCH_2). ^{31}P NMR (161.7 MHz, acetone-d_6, 25 °C): δ 81.2 (m, $^1J_{PtP}$ = 3643 Hz). ^{19}F NMR (376.05 MHz, acetone-d_6, 25 °C): δ −79.9 (s, 12F; $CF_2C\mathbf{F}_3$), −111 to −114 (overlapping ABX multiplets, 8F; $C\mathbf{F}_2CF_3$).

(dfepe)Pt(η^2-C_2F_4) (3). One atm of C_2F_4 was admitted to a 25 mL flask containing 0.100 g (0.0656 mmol) of **1** and 10 mL of acetone at ambient temperature. Initially yellow-brown, the solution became light orange after 5 min. After 30 min, all volatiles were removed, the residue was taken up in *ca*. 5 mL of ether, and the resulting white precipitate was isolated by filtration and dried under vacuum. Yield: 0.050 g (44%) of analytically pure **3**. Anal. Calcd for $C_{12}H_4F_{24}P_2Pt$: C, 16.74; H, 0.47. Found: C, 16.77; H, 0.37. ^{1}H NMR (400 MHz, acetone-d_6, 25 °C): δ 3.18 (m; PCH_2). ^{31}P NMR (161.7 MHz, acetone-d_6, 25 °C): δ 81.9 (m, $^1J_{PtP}$ = 2223 Hz). ^{19}F NMR (376.05 MHz, acetone-d_6, 25 °C): δ −79.7 (s, 12F; $CF_2C\mathbf{F}_3$), −109 to −112 (overlapping ABX multiplets, 8F; $C\mathbf{F}_2CF_3$), −125.8 (t, J_{PF} = 43 Hz, $^2J_{PtF}$ = 297 Hz, 4F; η^2-C_2F_4).

(dfepe)Pt(CO) (4). One atm of CO was admitted to a 25 mL flask containing 0.180 g (0.138 mmol) of **1** and 10 mL of acetone at ambient temperature. After 5 min, the solution became light yellow and all volatiles were removed. The residue was dissolved in *ca*. 5 mL of ether, and the solution was cooled to −78 °C; after 30 min, a light brown precipitate (0.050 g, 27%) was isolated by cold filtration and dried under vacuum. Although **4** isolated in this fashion was the sole (dfepe)Pt species observed by IR and ^{31}P NMR, an elemental analysis was not carried out because of decomposition in the solid state. IR (acetone, cm^{-1}): 2044 (s), 1296 (s), 1227 (s), 1120 (m), 961 (w), 748 (w). ^{1}H NMR (400 MHz, acetone-d_6, 25 °C): δ 2.72 (m; PCH_2). ^{31}P NMR (161.7 MHz, acetone-d_6, 25 °C): δ 78.1 (m).

(dfepe)Pt(CO)$_2$ (5). Treatment of acetone solutions of **1** with 2 atm of CO quantitatively afforded **5**, as judged by IR and NMR data. IR (acetone, cm^{-1}): 2073 (s), 2039 (s), 1297 (m), 1226 (s), 1095 (m), 960 (w), 807 (m). ^{1}H NMR (400 MHz, acetone-d_6, 25 °C): δ 2.81 (m; PCH_2). ^{31}P NMR (161.7 MHz, acetone-d_6, 25 °C): δ 52.6 (m, $^1J_{PtP}$ = 4150 Hz).

Electrochemical Studies. Cyclic voltammetry experiments were performed under an argon atmosphere for complex **1** and $[(^tBu)_2PCH_2CH_2P(^tBu)_2Pt(H)]_2$ using a EG&G Princeton Applied Research 273A potentiostat/galvanostat controlled by PAR Model 270/250 electrochemistry software (version 4.10). Measurements were taken at a platinum disk working electrode in CH_2Cl_2 with 0.1 M $[Bu_4N]^+ClO_4^-$ as the supporting electrolyte. IR compensation was not applied; although the observed peak separations were considerably larger than expected for a fully reversible redox couple (130 mV at 100 mV s^{-1}), linear plots of (scan rate)$^{1/2}$ versus peak current were satisfactorily linear (R^2 = 0.999). The $E_{1/2}$ value of +0.63 V for **1** was operationally referenced to $Ag/AgOTf_{sat}$ and corrected to SCE using a ferrocene/ferrocenium couple as a common internal standard (+0.465 V vs SCE).

DSC Studies. Measurements were carried out using a Perkin-Elmer DSC2 instrument. In a typical run, 12.5 mg of **1a** was placed in an aluminum sample pan. At a scan rate of 20 °C min^{-1}, the onset of an exothermic transition was observed at 365.0 K, with a maximum at 368.4 K. The enthalpy of this transition was found to be 510 J/mol.

Crystal Structure of [(dfepe)Pt(μ-H)]$_2$ (1a). X-ray data were collected on a Siemens R3m/V automated diffractometer system. The radiation used was Mo Kα monochromatized by a highly-ordered graphite crystal. The parameters used during the data collection are summarized in Table 1. All computations used the SHELXTL/IRIS (version 5.0) program library (Siemens Corp., Madison, WI). A suitable crystal of **1a** was grown from benzene at 3 °C. *C*-centered monoclinic unit cell dimensions were derived from a least-squares fit of 50 random reflections (18° < 2θ < 28°). Data were collected using the Wyckoff scan technique with a variable scan rate of 4.0−30.0°/min. Two standard reflections monitored after every 100 data collected showed no systematic variation. *C*2/*c* symmetry deduced from a statistical analysis of all collected data was confirmed by successful refinement in this space group. Data were corrected for absorption using the empirical program XABS2.[19]

The molecular structure of **1a** was solved using the SHELXTL direct methods program; all non-hydrogen atoms were located on a series of difference Fourier maps. Chelate backbone hydrogen atom positions were added in ideal calculated positions with d(C−H) = 0.96 Å and with fixed isotropic thermal parameters set at 1.2 times the isotropic equivalent of the attached carbon atom. All non-hydrogen atoms were refined anisotropically. Since examination of difference Fourier maps did not reveal residual electron density in chemically reasonable positions that could be attributable to hydride atom positions, hydride ligands were not included in the final refinements. Full-matrix least-squares refinement on F^2 gave an R_w^2 value of 19.70% for all data, with a corresponding value of R of 6.70% for 3253 data with $I > 2\sigma(I)$. The final difference Fourier map showed residual peaks of 3.71 and −4.39 e/Å^3 in the region between the platinum centers due to uncompensated absorption and residual hydride density.

Crystal Structure of [(dfepe)Pt(μ-H)]$_2$ (1b). X-ray data were collected as described above. The parameters used during the data collection are summarized in Table 1. All computations used the SHELXTL/IRIS version 4.2 set of programs. A suitable crystal of **1b** was grown from dichloromethane at −50 °C. Orthorhombic unit cell dimensions were derived from a least-squares fit of 50 random reflections (18° < 2θ < 28°). Data were collected using the Wyckoff scan technique with a variable scan rate of 4.0−30.0°/min. Two standard reflections monitored after every 100 data collected showed no systematic variation. *Pccn* symmetry deduced from a statistical analysis of all collected data was confirmed by successful refinement in this space group. Data were corrected for absorption using the empirical program XABS2.

The molecular structure of **1b** was solved using the SHELXTL direct methods program; all non-hydrogen atoms were located on a series of difference Fourier maps. Chelate backbone hydrogen atom positions were modeled as described above. All non-hydrogen atoms were refined anisotropically. Hydride ligands were not located and were excluded from the final refinement model. Full-matrix least-squares refinement on F gave an R value of 4.23% (R_w = 4.87%) for 3073 data with $I > 2\sigma(I)$. The final difference Fourier map showed residual peaks of 1.62 and −1.23 e/Å^3 in the region between the platinum centers.

Acknowledgment. We thank Prof. R. A. Andersen for supplying a sample of $[(^tBu)_2PCH_2CH_2P(^tBu)_2Pt(H)]_2$ for comparative study and for helpful discussions. We also thank Prof. D. G. Nocera for helpful discussions. This work was supported by the National Science Foundation (Grant No. CHE-9310550). Johnson Matthey is also gratefully acknowledged for a generous loan of platinum chloride.

Supporting Information Available: Tables giving structure determination details, atomic positional parameters, bond distances and angles, thermal displacement parameters, and hydrogen coordinates for **1a** and **1b** and figures illustrating representative electrochemical and DSC results for **1** (17 pages). Ordering information is given on any current masthead page.

IC960126Q

(19) Parkin, S.; Moezzi, B.; Hope, H. *J. Appl. Crystallogr.* **1995**, *28*, 53.